

# Analysis of the Effect of Spherical Texture on the Performance Characteristics of Journal Bearing using JFO Boundary Conditions

Nayab Rasool Syed, Sashindra Kumar Kakoty  
IIT, Guwahati, India

*Abstract: This paper's objective is to analyze textured bearings' performance for different texture geometric and bearing operating parameters in comparison to the plain bearing. The mass conserving (JFO) boundary conditions are implemented in solving governing Reynolds equation. The governing Reynolds equation is discretized using the central difference method. From this numerical study, optimal texture and bearing geometric parameters are found corresponding to the maximum flow coefficient and minimum lubricant temperature change using performance enhancement ratio (PER). Also, it is found that the protruded textured bearing gives the best performance, when textured in the second half textured region configuration, compared to dimple textured bearing and untextured bearing.*

*Keywords: surface texture; journal bearing; JFO boundary conditions; PMD method; performance enhancement ratio*

## I. INTRODUCTION

Textured bearings are being investigated more in recent times than it was a decade ago. It is because that texturing the surface of the bearing improves the bearing performance. The regular surface texture in the form of micro-dimples/protrusions has pre-defined parameters for texture such as depth/height and area density. There are different manufacturing techniques to produce different types of texture geometry on the surface of the bearings such as laser surface texturing (LST), photolithography, chemical etching and few mechanical techniques like vibro-rolling and milling, etc. But, the poor choice of geometry and distribution of texture may give reduction in the performance of the bearing. So, it is important for a designer, to choose the better geometry and distribution of texture that improves performance of the bearing. Therefore, various researchers have conducted investigations to study the impact of various texture shapes on the bearing when its inner surface is textured. Brizmer et al.[1] theoretically studied the LST impact on the parallel thrust bearing. The optimum parameters for the dimples have been found to attain the maximum load capacity. The authors have also found the best mode of LST for maximum load capacity. The experimental study has also been carried out by Etsion et al. [2] on the impact of LST on the performance parameters of parallel thrust bearing, in terms of clearance and friction.

Brizmer and Kligerman [3] have conducted a theoretical study on the implementation of LST on the journal bearings. The authors have analyzed the effect of full-LST and partial-LST on the load-carrying capacity and attitude angle of the journal bearing. They have found the favorable mode of LST and optimum parameters of dimple texture for maximum load bearing capacity. Syed and kakoty [4] have conducted performance analysis on textured bearings using mass conserving model. They found that dimple textured bearing gives better load capacity when textured in the second half of circumference compared to protrude textured and plain bearing. It is observed from literature that incorporating the textures on the surface of the bearing enhances its performance. However, right selection of shape, size, depth, and location is essential. Therefore, the objective of the present paper is to compare the impact of spherical dimple and protruded texture on the static performance characteristics of journal bearing such as flow coefficient and lubricant temperature change. Hence, in this work, the effect of texture distribution, dimple depths, texture heights and eccentricity ratios on the spherical dimple and protruded textured bearings are investigated. Mass conserving (JFO) boundary conditions have been implemented in the solution of governing Reynolds equation using the central difference method. The PMD method that has been proved to be computationally efficient compared to the

multigrid method for the textured journal bearing problem [5], has been implemented to attain the converged fractional film content parameter ( $\theta$ ) results and thus the pressure results.

## II. THEORETICAL ANALYSIS

### A. Governing equation

The governing Reynolds equation for the journal bearing operating at steady state condition can be written as:

$$\frac{\partial}{\partial x} \left( \rho h^3 \frac{\partial p}{\partial x} \right) + \frac{\partial}{\partial z} \left( \rho h^3 \frac{\partial p}{\partial z} \right) = 6\eta U \frac{\partial \rho h}{\partial x} \dots(1)$$

The universal Reynolds equation that is applicable for mass-conservation boundary conditions can be referred from the work of Fesanghary and Khonsari [6]. The fluid film thickness can be referred from Brizmer and Kligerman [3].

### A. Non-dimensional Bearing Parameters

Following the general non-dimensionalization available in literature, the pressure and the fluid film thickness in dimensionless form can be obtained as follows:

$$\bar{p} = \frac{pC^2}{\eta UR} \quad (2)$$

$$\bar{h} = \frac{h}{C} \quad (3)$$

Here, dimensionless coordinates are  $\bar{x} = \frac{x}{R}$  and

$$\bar{z} = \frac{z}{L}$$

The dimensionless flow can be obtained from the equation below:

$$\bar{Q} = -\frac{1}{12} \left( \frac{D}{L} \right)^2 \int_0^{2\pi} \bar{h}^3 \frac{\partial \bar{p}}{\partial z} d\psi \quad (4)$$

The dimensionless temperature change is found from the following equation:

$$\Delta \bar{T} = \gamma \left( \frac{\eta UL}{J \rho s C^2} \right) f \frac{\bar{W}}{\bar{Q}} \quad (5)$$

Where  $J \rho s = 1.7 \times 10^6$  in SI units.

### C. Performance enhancement ratio

In the present study, the performance enhancement ratio (PER) is defined as presented below:

$$PER = \frac{\left( \frac{\text{Flow coefficient of textured bearing}}{\text{Flow coefficient of untextured bearing}} \right)}{\left( \frac{\text{Temperature change of textured bearing}}{\text{Temperature change of untextured bearing}} \right)} \quad (6)$$

## III. RESULTS AND DISCUSSION

The friction coefficient results obtained using PMD method (with 3 levels) for one sectorial segment (simplified to parallel slider) of textured parallel thrust bearing are compared with the experimental results of Etsion et al. [2], for varying load at a speed of 1500 rpm, as illustrated in Fig. 1. The comparison is done for unidirectional texturing ( $L/B = 0.75$ ,  $p_s = 0.6$  and  $\alpha = 0.734$ ) and bidirectional texturing ( $L/B = 0.75$ ,  $S_p = 0.614$  and  $\alpha = 0.633$ ). Since the trends of the present results for friction coefficient are similar to that of the experimental results, therefore, the codes developed are used for analysis of textured journal bearing after modification. The input parameters used for the validation are slider width  $B = 50$  mm, dimple base radius ( $p_r$ ) = 30  $\mu\text{m}$ , dimple depth ( $p_h$ ) = 6.5  $\mu\text{m}$ , viscosity ( $\eta$ ) = 0.001 Pa. s, speed = 1500 rpm, velocity ( $U$ ) = 4.9 m/s, Bulk modulus ( $\beta$ ) = 2.1 GPa, cavitation pressure ( $c_p$ ) = 0.9 bar, ambient pressure ( $a_p$ ) = 1 bar.

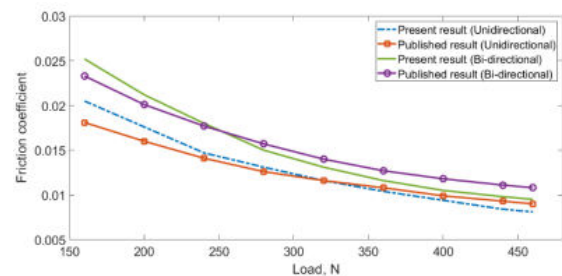


Figure 1: Validation of the present results with those of Etsion et al. [2]

In the present study, the protruded and dimple textured bearing performance characteristics such as flow coefficient and lubricant temperature change are estimated for different texture depth/height with various eccentricity ratios. The different eccentricity ratios considered here are 0.2, 0.4 and 0.6. The different textured region configurations of texturing, in circumferential region of journal bearing, that have been considered in this study are full textured region ( $0^\circ - 360^\circ$ ), first-half textured region ( $0^\circ - 180^\circ$ ) and second-half textured region ( $180^\circ - 360^\circ$ ). In this study, the 3-level situation of PMD method is implemented with mesh sizes for level 1, level 2 and level 3 as  $28 \times 9$ ,  $56 \times 18$  and  $112 \times 36$ , respectively. The ultimate convergence criterion followed is  $10^{-5}$ . The parameters, for journal bearing with spherical dimple and protruded textures, that are considered in the present analysis are diameter ( $D$ ) = 62.8 mm, length-to-diameter ratio ( $L/D$ ) = 1, clearance ( $C$ ) = 0.055 mm, dimple

base radius (  $r$  ) =10 mm, dimple area density (  $p$  S ) =0.3, viscosity (  $\eta$  ) =0.0035 Pa. s, velocity (  $U$  ) =19.7 m/s, Bulk modulus (  $\beta$  ) =0.1 GPa, cavitation pressure (  $c$  p ) =0.9 bar, ambient pressure (  $a$  p ) =1 bar, Viscosity-temperature index (  $\gamma$  ) =0.1, gfactor =0.8.

### Fully textured region configuration ( $0^\circ - 360^\circ$ )

For the analysis of fully textured region distribution, two rows of 6 textures in circumferential direction of journal bearing are considered for spherical dimple and protruded textures. From Figs. 2(a) to (c), it is depicted that there is increment in flow coefficient for fully textured journal bearing with dimple textures and fully textured journal bearing with protruded textures with an increment in the texture depth/height value when compared to the plain journal bearing. From Figs. 2(d) to (f), it is shown that there is decrease in temperature change of lubricant for fully textured journal bearing with dimple textures and fully textured journal bearing with protruded textures with an increment in the texture depth/height value when compared to the plain journal bearing.

### First Half-Textured Region Configuration ( $0^\circ - 180^\circ$ )

In the analysis of first half-textured region configuration, two rows of 3 textures in first-half circumferential region of journal bearing are selected for spherical dimple and protruded textures. From Figs. 3(a) to (c), it is depicted that there is increment in flow coefficient for journal bearing with dimple textures and decrement in flow coefficient for journal bearing with protruded textures with an increment in the texture depth/height value when compared to the plain journal bearing. From Figs. 3(d) to (f), it is shown that there is decrement in temperature change for journal bearing with dimple textures whereas, increment in temperature change for journal bearing with protruded textures with an increment in the texture depth/height value when compared to the plain journal bearing.

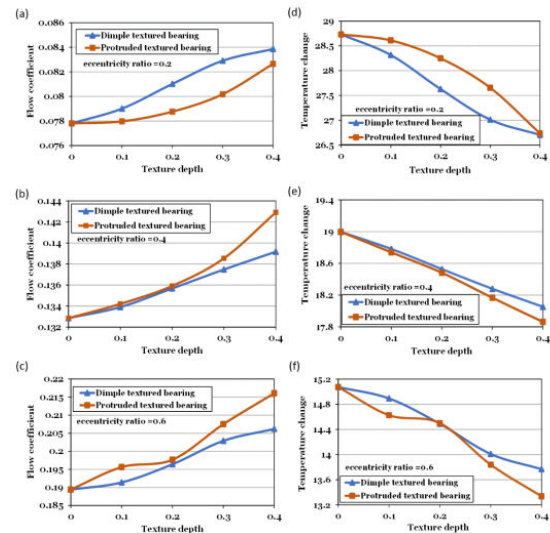


Fig. 2: Comparison of flow coefficient and temperature change for journal bearing with dimple and protruded textures with untextured bearing by varying texture depth for full textured region configuration

### Second Half-Textured Region Configuration ( $180^\circ - 360^\circ$ )

In the present analysis of second half-textured region configuration, two rows of 3 textures in second-half circumferential region of journal bearing are selected for spherical dimple and protruded textures. It is depicted from Figs. 4(a) to (c) that there is increment in flow coefficient for journal bearing with protruded textures and reduction in flow coefficient for journal bearing with dimple textures with an increment in the texture depth/height value when compared to the plain journal bearing. From Figs. 4(d) to (f), it is depicted that there is decrement in temperature change for journal bearing with protruded textures and increment in temperature change for journal bearing with dimple textures with an increment in the texture depth/height value compared the plain journal bearing.

### Calculation of Optimum Design Parameters

The performance enhancement for journal bearing with spherical dimple and protruded textures corresponding to load capacity and friction variable is obtained by performance enhancement ratio (PER) using eqn. 6 for each case of texture depth/height considered in every eccentricity ratio in all three texturing configurations (  $0^\circ - 360^\circ$ ,  $0^\circ - 180^\circ$  and  $180^\circ - 360^\circ$  ) to find optimal texture depth/height and area for which the flow

coefficient is maximum and the temperature change is minimum. It is found that PER maximum value for journal bearing with protruded textures and journal bearing with dimple textures as 1.289413 and 1.191759, respectively at the eccentricity ratio of 0.6 and the texture height/depth of 0.4 for fully textured region configuration. Further, it is observed for first-half textured region, the PER maximum value for journal bearing with protruded textures is 0.995036 at the texture height of 0.1 and at the eccentricity ratio of 0.6 and for journal bearing with dimple textures as 1.21571 at the eccentricity ratio of 0.2 and the dimple depth of 0.4. Furthermore, for second-half textured region, it is noticed that the PER maximum value for journal bearing with protruded textures is 1.563438 at the eccentricity ratio of 0.2 and the texture height of 0.4 and for journal bearing with dimple textures is 1.000283 at the eccentricity ratio of 0.6 and the dimple depth of 0.1.

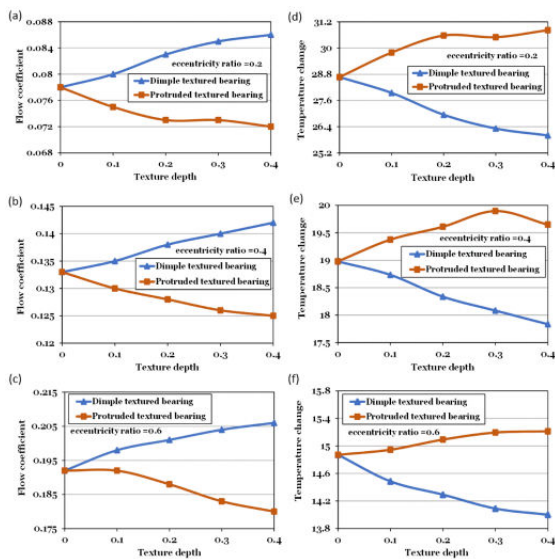


Fig. 3: Comparison of flow coefficient and temperature change for journal bearing with dimple and protruded textures with untextured bearing by varying texture depth for first-half textured region configuration

#### IV. CONCLUSIONS

In this study, the journal bearing's performance characteristics with dimple and protruded spherical textures on its surface has been compared to determine the optimal texture depth/height, texturing region and eccentricity ratio for the maximum flow coefficient and minimum lubricant temperature change. The

governing Reynolds equation has been solved considering JFO boundary conditions using PMD method. The conclusions that are drawn from the present study are presented below. The protruded textured journal bearing gives best performance in terms of maximum flow coefficient and minimum temperature change when textured with spherical protuberances in the second half textured region configuration compared to the spherical dimple textured journal bearing and plain journal bearing irrespective of any texture region configuration. The optimum operating and texture parameter values corresponding to maximum flow coefficient and minimum temperature change are eccentricity ratio of 0.2 and the texture height of 0.4.

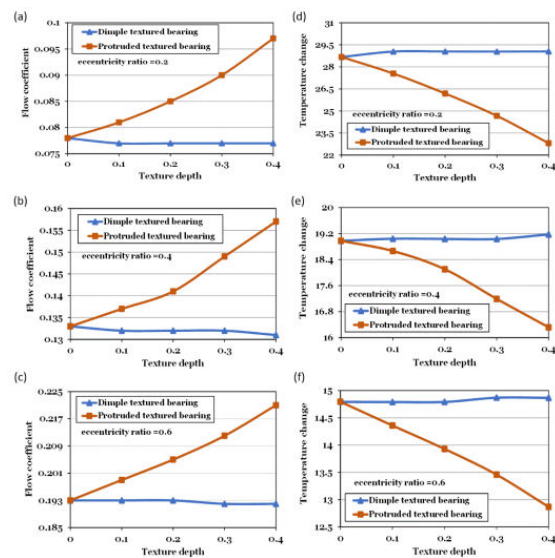


Fig. 4: Comparison of flow coefficient and temperature change for journal bearing with dimple and protruded textures with untextured bearing by varying texture depth for Second-half textured region configuration.

#### REFERENCES

- [1] Brizmer, V., Kligerman, Y. and Etsion, I. (2003), "A laser surface textured parallel thrust bearing", Tribology transactions, Vol. 46 No. 3, pp. 397-403. doi.org/10.1080/10402000308982643
- [2] Etsion, I., Halperin, G., Brizmer, V. and Kligerman Y. (2004) "Experimental investigation of laser surface textured parallel thrust bearings", Tribology Letters, Vol. 17 No. 2, pp. 295-300. doi.org/10.1023/B:TRIL.0000032467.88800.59
- [3] Brizmer, V., and Kligerman, Y. (2012), "A Laser Surface Textured Journal Bearing," Journal

of Tribology, Vol. 134 No. 3, pp. 1–9.  
doi.org/10.1115/1.4006511

[4] Syed, N.R. and Kakoty, S.K. (2022),  
“Influence of spherical protruded and dimple  
texture on the journal bearing performance: A  
comparative theoretical analysis implementing  
JFO boundary conditions,” Industrial Lubrication  
and Tribology, (ahead-of-print).  
<https://doi.org/10.1108/ilt-04-2022-0115>

[5] Syed, N.R. and Kakoty, S.K. (2021),  
“Computational efficiency improvement of  
dimple textured hydrodynamic journal bearing  
using progressive mesh densification method”,  
Journal of Tribology, Vol. 144 No. 3.  
doi.org/10.1115/1.4051039

[6] Fesanghary, M. and Khonsari, M. M. (2011),  
“A Modification of the Switch Function in the  
Elrod Cavitation Algorithm,” Journal of  
Tribology, Vol. 133 No. 2, pp. 1–4.  
doi.org/10.1115/1.4003484.